A Molecular View of Lipid-mediated Activation Process of Apolipoprotein E

Dube Dheeraj Prakashchand and Jagannath Mondal*

Tata Institute of Fundamental Research, Center for Interdisciplinary sciences, Hyderabad 500107, India

E-mail: jmondal@tifrh.res.in,+914020203091

Abstract

Apolipoprotein E (ApoE) is a major determinant protein of lipid-metabolism and actively participates in lipid transport in plasma and central nervous system. As a part of its lipid-transport activity, low-density-lipid receptor (LDLR) needs to recognise apoE as a ligand. But, all prior evidences point to the fact that the recognition of apoE by LDLR only takes place in presence of lipid molecules which are assumed to play an important role in conformationally activating apoE upon binding. However, the molecular mechanism underlying the complexation process of apoE with lipid molecules and associated lipid-induced conformational change of apoE are currently elusive. Here we capture the spontaneous complexation process of monomeric apoE3 and phospholipid molecules by employing molecular dynamics simulation at multiple resolution. In particular, our multi scale simulations demonstrate a large-scale conformational change of the full-length apoE3, triggered by two-stage apoE-lipid complexation process. At first stage, lipid molecules assemble close to C-terminal domain of the protein and induce a rapid separation of C-terminal domain of monomeric apoE3 from rest of its tertiary fold. In the second and final stage, long-time scale simulation captures a slow *on-the-fly* lipid-induced inter-helix separation process in N-terminal domain of the protein. The

resultant equilibrated complex, as obtained in the current work resembles an 'open conformation' of lipid-stabilised apoE, previously hypothesised based on small-angle X-ray scattering experiments. Taken together, the simulations provide a molecular view of kinetic interplay of apoE and lipid complexation multi-stage process leading to conformational changes in protein, potentially making it conducive for recognising LDLR.

Introduction

The intense hydrophobic character of triglycerides and cholesterol prevents them from getting dissolved in the aqueous environment of the blood. These hydrophobic entities are transported in blood plasma in the form of large assemblies of lipids (like phospholipids, triglycerides, cholesterol-esters and free-cholesterol) and proteins called lipoproteins.[1,2] Each of these lipoproteins carry different proteins serving as address tags which decide the destination and hence the function of each lipoprotein complexes. Apolipoprotein E (ApoE), a 299-residue protein consisting of N-terminal domain and C-terminal domain connected by a hinge-region,[3–5] constitutes the protein component of lipoproteins not only in plasma[6] but also in the central nervous systems (CNS)[7–10] and serves as one of the major determinants in lipid metabolism.[11] Fine-tuned proportions of the correct allelic[12–14] form of apoE is key towards preventing conditions like type III hyperlipoproteinemia[15–20] and build-up of plasma cholesterol and most importantly, has pathological consequences in a variety of neurological disorders including Parkinson's disease and Alzheimer's disease.[21–28] Poor lipid transport in the plasma and in the CNS is directly correlated with apoE polymorphism.[29–32]

As a part of its lipid-transport activity, low-density-lipid receptor (LDLR) recognises apoE as a ligand. However, in absence of lipid molecules, the apoe3 is not recognised by LDLR. Prior experimental investigations indicate that as a prerequisite for apoE binding to the Low density lipid receptor (LDLR),[33–35] apoE needs to be conformationally activated via remaining associated with lipid for the most part.[36–39] It has also been demonstrated that

the complexation with phospholipids to form discoidal structures gives rise to a apoE.lipid particle that binds efficiently to the LDL receptor.[40] More over, full-length apoE has been found to bind to LDL receptors on fibroblasts only after complexation with lipid.[41] All these circumstantial evidences point to the fact that the receptor recognition properties of this protein are manifested only in a lipid-associated state. However, a molecular-level insight into the mechanism associated with ApoE-lipid complexation process and plausible morphology of apoE-lipid complex are currently elusive. In the current article, we resolve a molecular picture of conformational reorganization of apoE upon apoE3-phospholipid complexation process, by combination of all-atom and coarse-grained Molecular Dynamics simulations.

Over the years, model lipoproteins composed of apoE and phospholipids have served as a suitable in-vitro mimic of many of the critical biological activities of naturally occurring apoE-containing lipoproteins.[42] A series of biophysical and spectroscopic studies have brought out interesting features about the interactions of apoE and phospholipids.[43–47] Past investigations have essentially converged on the notion that the C-terminal domain of the apoE is the initial and major lipid binding domains.[43,46–50] Garai and co-workers, using fluorescence-based kinetic studies, have illustrated that while all lipid-free isoforms exist primarily as monomers, dimers and tetramers at micro molar concentration, lipid binding takes place only with the monomeric form of apoE.[44] Perugini and coworkers also have also earlier inferred that monomeric form of apoE prevails on lipoprotein surface.[45]

Phospholipids, including dimyristoylphosphatidylcholine (DMPC) or dipalmitoylphosphatidylcholine (DPPC) have been used to create nanometer scale protein-lipid complex wherein the apolipoprotein circumscribes the periphery of a disk-shaped phospholipid bilayer.[42,51] On the basis of biophysical and spectroscopic studies, various models of ApoE-phospholipid complexes have been proposed.[4,51–53] These models basically suggest possible ways in which the N-terminal helix bundle may change its structure upon lipid association. Small angle X-ray scattering (SAXS) based investigations of morphological features of apoE-DPPC complex by Weisgraber and coworkers have proposed that these complexes

are ellipsoidal in shape and the morphology of the phospholipid core is compatible with a twisted-bilayer model.[42] The same group however has crystallized apoE-DPPC complex at a 10 angstrom resolution and predicted an incomplete toroidal model.[54] While the general consensus is that the protein undergoes a lipid binding-induced conformational change, ultimate conformation adopted by apoE in presence of phospholipids is still unknown. This is mostly due to the lack of clarity about the nature of a molecular-level conformational change that apoE undergoes in the process of lipid binding.

The report of a high-resolution NMR structure of the full-length monomeric mutant of apoE3 by Chen et al[55] has rejuvenated the call for a molecular-level hypothesis on apoE3-lipid interaction and associated conformational organisation that the apoE3 might possibly undergo upon lipid association. By combining existing hydrogen-deuterium exchange data and via inferring from NMR-derived structure and non-equilibrium computer simulations, Frieden and coworkers have proposed possible mechanisms of conformational organisation of ApoE3 via lipid binding in between N-terminal and C-terminal domain and suggested that the presence of hinge region[56] and salt-bridges between N-terminal and C-terminal play an important role in the complexation process.[57] However, an atomic-level picture of the dynamical process of lipid-induced conformational organisation associated with apoE.phospholipid complexation process is yet to emerge. The current work closes this gap by capturing the phospholipid binding-induced conformational change of apoE3 via extensive molecular dynamics simulations. Specifically, by utilising both all-atom and coarse-grained model we report a high-resolution dynamical picture of apoE3-DPPC complexation process in explicitly modelled water at two different time scales. First, we show that the C-terminal domain of monomeric apoE3[55] moves away from N-terminal domain in presence of DPPC lipids, within the period of our atomistic MD simulation. The atomistic simulations identify the important regions of protein where the lipids settle. The trajectories elucidate the key local changes in the helicity, salt-bridges and intrinsically disordered regions of apoE3 as a consequence of lipid binding. In the subsequent step, we adopt coarse-grained models and

demonstrate the slow *on-the-fly* unwinding of N-terminal domain upon lipid association and provide a high-resolution picture of the apoE3-lipid complex.

Results and Discussion

The precedent experimental investigations have established that the apoE3 binds with phospholipid in its monomeric form.[44] Accordingly, the current computer simulations focus on elucidating the mechanism of lipid complexation with monomeric apoE3. As would be unfolded by our investigations, we demonstrate the kinetic molecular picture of overall complexation process occurring in two major steps: (I) In a first rapid step, lipid induces separation of C-terminal domains of apoE3 (II) In the final step, a slow unwinding of N-terminal domain of ApoE3 takes place. In the current article, we employ all-atom and coarse-grained molecular dynamics simulations respectively, to access the time scale associated with these two steps and provide a molecular view of the spontaneous ApoE3-lipid complexation process. The simulated lipid bound conformation, represented in figure 6 is majorly stabilised by the strong hydrophobic association between lipids and reorganised N- and C-terminal domain.

1. Lipid induced separation of C-terminal domain of ApoE as the first step

1A. Preferential lipid-accumulation around ApoE3 C-terminal domain: The NMR derived structure of monomeric apoE3 by Chen et al[55] forms the basis of our work for exploring its mechanism of interaction with lipid molecules. Following previous works,[55,57] we define residues 1-167 as N-terminal domain, residues 206-299 as C-terminal domain and residues 168-205 as the hinge helix region. The monomeric apoE3 in its all-atom representation is solvated with water and 135 DPPC lipid molecules are randomly placed inside a cubic box of 11.9 nm. Figure 1a depicts a snapshot of the initial configuration of the system. Multiple realisations of initial configuration of the system, thus prepared, are individually subjected to

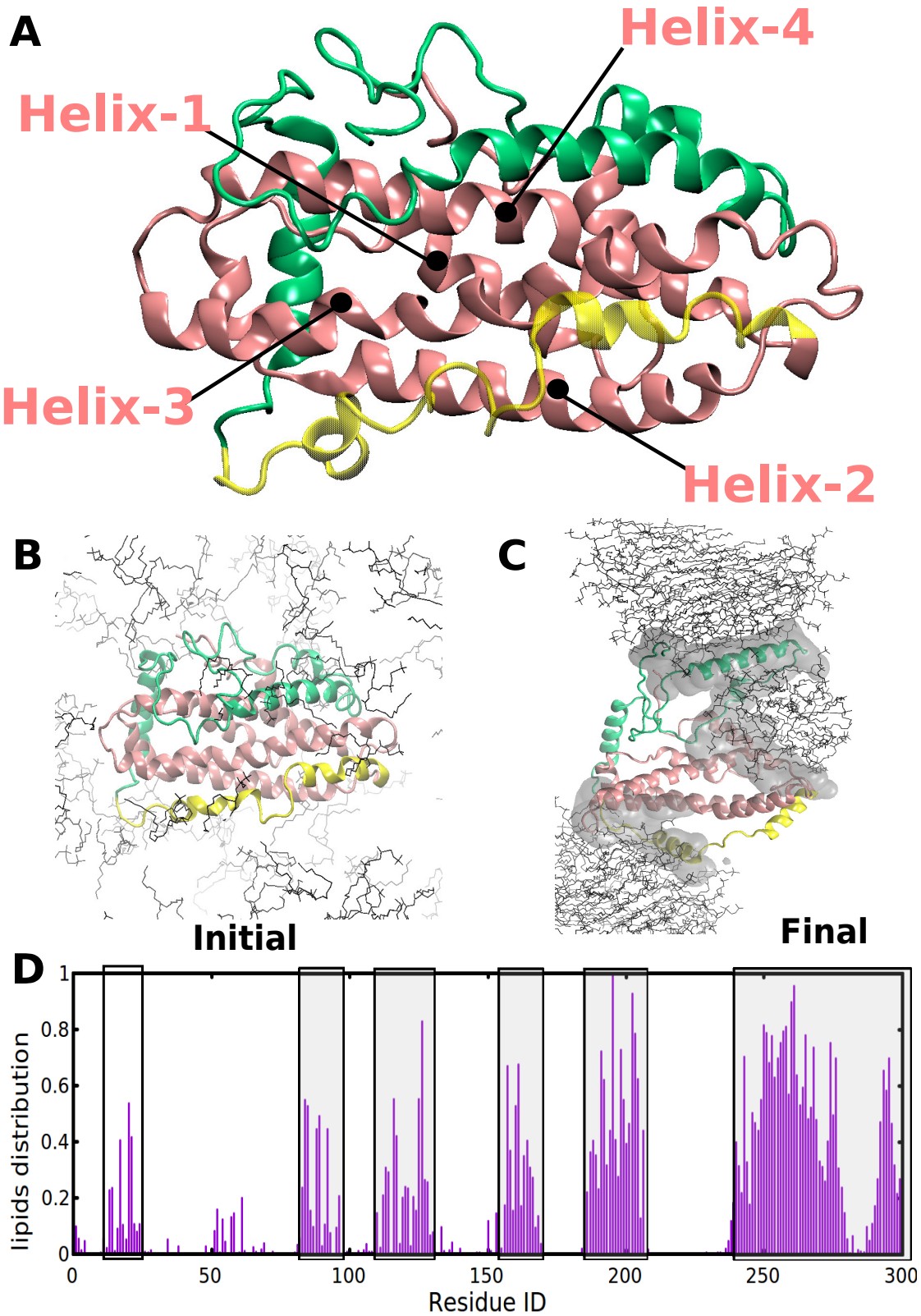

Figure 1: **a.** Snapshot of apoE3 with NT domain marked as pink; the hinge region in yellow ; and the CT domain shown as green. The four helices of NT domain helical bundle are also pointed out. Two all-atom simulation snapshots show the spatial distribution of the lipids around the protein at different time points: **b.** in the beginning of the simulation and **c.** a representative snapshot of apoE3 in the lipid-equilibrated phase of the simulation. Water not shown for clarity. **d.** Normalised probability of distribution of lipids around around each of the residues of apoE3.

multi-microsecond long equilibrium MD simulations at temperature of 320 K. As depicted in supplemental movie S1 (See link `https://www.dropbox.com/s/sg6igroy6u87hef/movie_S1.mp4?dl=0`), we find that lipid molecules diffuse from the bulk media and assemble around the protein during the time scales of these microsecond-long simulations. Figure 1b illustrates the representative snapshot of equilibrated conformation of apoE3 in presence of of DPPC lipids, as obtained at the end of 2 microsecond-long MD simulation. We find that the lipid molecules eventually get settled mostly near the C-terminal domain of the monomeric apoE3. The spatial density map of the lipid molecules around protein, averaged over the simulation trajectories, also indicates a localised accumulation of lipid molecules near the C-terminal domain (see grey coloured density map around C-terminal domain in figure 1b). Figure 1c plots the statistical propensity of lipid accumulation within 0.5 nm cutoff distance of each constituent residue of apoE3, averaged over all simulation trajectories. Consistent with spatial density profile, we find that large segments of C-terminal domain (residues 243-296) are mostly surrounded by lipids, while there are also isolated locations around N-terminal domains (residues 13-24 , 84-97, 108-130, 186-206) showing non-negligible lipid density. This result is consistent with previous experimental reports of preferential lipid binding propensities by C-terminal domain of apoE.[43,46,47] Specifically, the C terminal domain presents a large exposed hydrophobic surface which acts as the initiator of interactions with lipids. The preferential binding of lipid molecules to the C-terminal domain of apoE3, as captured in these all-atom simulations, also resonates very well with the proposed hypothesis by Chen et al based on their NMR structure of monomeric apoE3.[55]

1B. Lipid-induced separation of C-terminal domain of apoE: As the most intriguing feature of the snapshot represented in the figure 1b, significant structural reorganisation of apoE3 tertiary fold is clearly evident due to phospholipid accumulations. Specifically the snapshot indicates that C-terminal domain of the apoE3 moves away from the rest of the protein's tertiary fold in presence of lipids. Figure 2 compares representative equilibrated snapshots of apoE3 in neat water with that in presence of phospholipid, as obtained near the

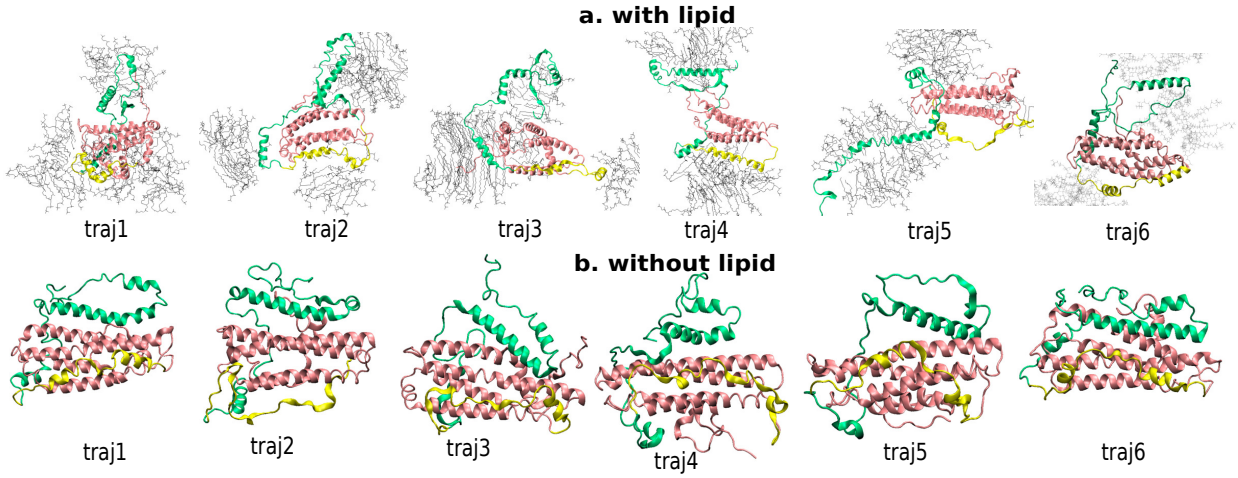

Figure 2: **a.** The representative snapshots obtained in multiple independent all-atom trajectories with simulation box containing 135 molecules of DPPC along with the water molecules (water not shown). **b.** The structures attained in multiple independent all-atom trajectories without any lipids molecules. Both types of simulations were run for similar length (2 microseconds) (refer to the color code described in the figure 1))

end of various (six trajectories for each cases) multi-microsecond long all-atom MD trajectories. Consistent with our earlier finding,[19] we find that the tertiary fold of apoE3 remains intact in neat water, contrary to that in lipid-water mixture. This comparison confirms that the conformational reorganisation of apoE3, as observed in the current simulation trajectories is caused due to presence of phospholipids and not as a result of thermal fluctuation. The supplemental movie S1 captures the dynamical process of conformational organisation that apoE3 undergoes in presence of lipid during 2 microsecond-long all-atom MD simulations. We find that C-terminal domain of apoE3 gradually moves away from the helix 3/helix4 interface of the N-terminal domain within microsecond-long time scale in majority of our simulation trajectories. On the other hand, the tertiary fold of N-terminal domain remains largely unperturbed within the time scale of our all-atom simulations. This lipid-induced structural change in protein, elucidated in figure 1b and figure 2, warrants a detailed molecular-level characterisation, as would be elaborated in the upcoming sections.

Figure 3a represents the time profile of root-mean-squared deviation (RMSD) of C-terminal domain, relative to the NMR-derived structure of apoE3. In line with the sup-

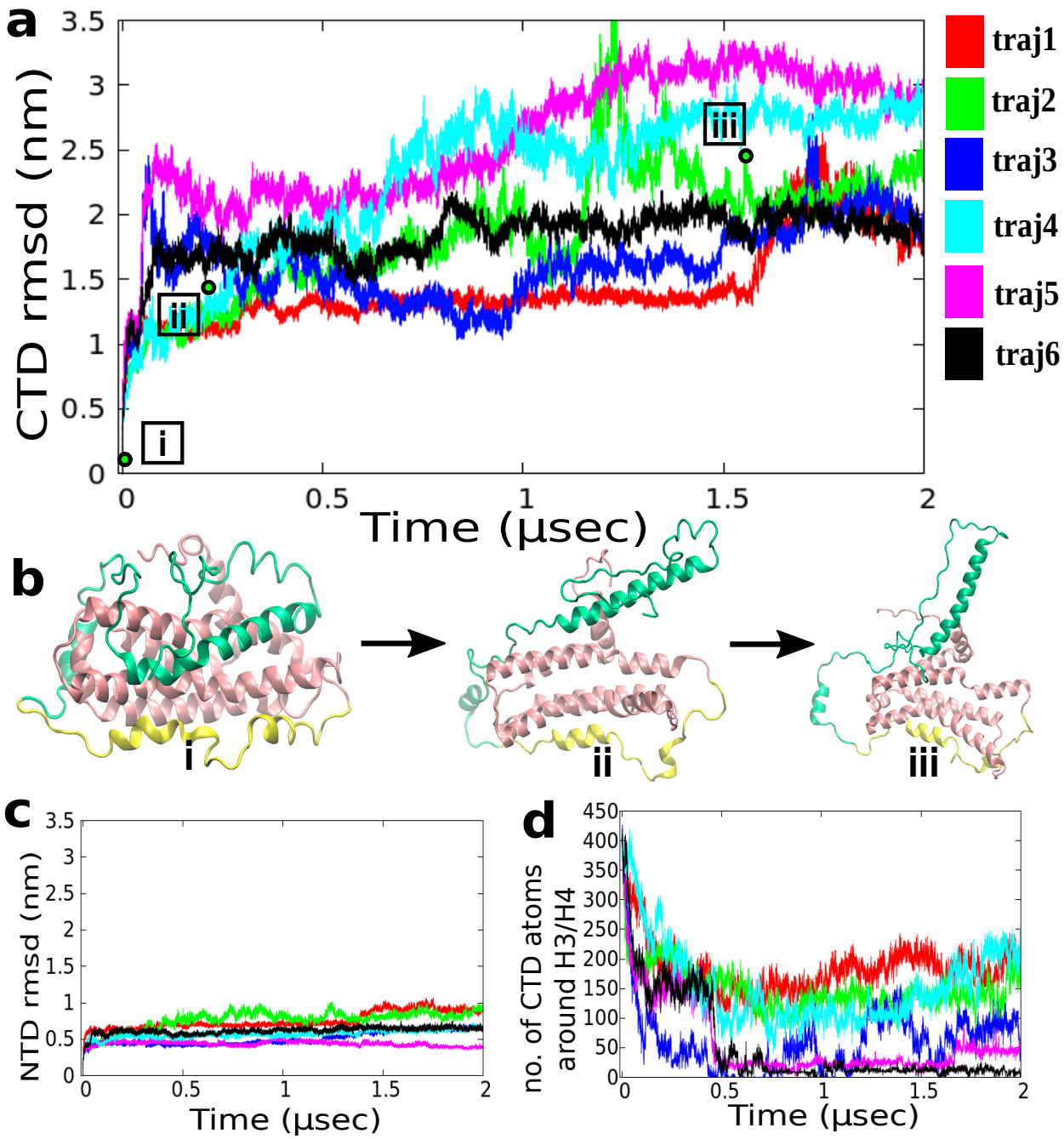

Figure 3: **a.** The time series of RMSD of C-terminal domain relative to NMR-derived structure of apoe3 (pdb: 2l7b)[55] (initial structure of the MD simulation) indicating large opening of the C-terminal domain(CTD). **b.** The snapshots at three time-points highlighted in part a of the figure. These snapshots indicate the closed CTD structure in the beginning of the simulation, the partly opened CTD structure and the fully opened CTD respectively (Refer to color code in figure 1 and 2). **c.** The time series of RMSD of N-terminal domain (NTD) indicating considerably weaker lipid-induced conformational change of the NTD within the 2 microsecond time-scale. **d.** The time series of the number of atoms of CTD crowding around the helices 3 and 4 of NTD. The less the crowding the more easy for it to open.

plemental movie S1 , we find that RMSD of the C-terminal domain (figure 3a) steadily increases with time and plateaus to a large value of 2.5-3 nm in majority of the MD simulation trajectories. The simulation-snapshots in figure 3b, extracted from key time-points of RMSD profile of C-terminal domain, illustrate the gradual progression of the unwinding process of the C-terminal domain of apoE3 away from N-terminal domain. On the other hand, the RMSD, relative to NMR structure, is relatively muted in N-terminal domain and ranges between 0.5-1 nm (figure 3c). This observation is consistent with the event of preferential lipid accumulation around C-terminal domain (see figure 1b). This observation from our simulation also supports Chen et al's[55] and Frieden et al's[57] hypothesis that N-terminal domain acts as the folding template of C-terminal domain in the NMR-derived structure of apoE3. Figure 4d plots the time profile of number of C-terminal domain atoms within 0.5 nm radial distances of Helices 3/4 of N terminal domain. We find that it acts as a sensitive parameter for characterising the extent of opening of the C-terminal domain in presence of lipid. As seen in this time profile of figure 3d, the number of neighbouring C-terminal atoms around (within a radius of 0.5 nm) the helix 3/4 of the N-terminal domain gradually reduces with time. As we would see in the later part of the article, this lipid-induced separation of C-terminal domains, away from the N-terminal domain, would provide an opening for eventual unwinding of N-terminal domain. Thus, the contacts lost between the C-terminal and N-terminal domains would be replenished by the contacts between lipids and the N-terminal domain.

1C. Lipid binding leads to disruption of apoE3 salt-bridges and Intrinsically disordered regions: Analysis of the computer simulated trajectories provides several key insights into the atomistic details of the structural changes due to lipid-induced unfolding of C-terminal domain. As shown in Figure S1 we find that the assembly of the lipid particles around the protein mostly retains the helicity of apoE3, except at few regions of C-terminal domains of protein. The comparison of residue-wise helicity of apoE3 in neat water with that in phospholipid-water mixture indicates that (figure S1) residues 238-245 (region 2) and

264-271 (region 3) loose helicity in presence of lipids while the helical propensity of 209-222(region 1) increases. However, the secondary structures of majority of the protein remain unaltered even in presence of the protein.

Inspection of the simulation trajectories reveal that the lipid assembly around the protein disrupts several salt-bridge interactions between N and C-terminal domains. The presence of these salt-bridges had been earlier reported by Chen et al[55] as one of the stabilising factors of monomeric apoE3. As shown in figure 4a, there are five main salt-bridges establishing contacts between C-terminal domain and helices 2/3 of N-terminal domain in aqueous medium: salt-bridge region labelled 1 is a pair of salt-bridges closely packed together consisting of 217ARG-50GLU and 213ARG-49GLU ; similarly other salt bridges are characterised as follows 2:233LYS-132GLU , 3: 238GLU-114ARG and 242LYS-110ASP , 4: 255GLU-95LYS and finally 5: 262LYS-88GLU. Our simulation confirms that these salt-bridges remain mutually intact in absence of lipids (see left panel in figure 4a). However, analysis of our simulation trajectories in presence of lipids predicts that the salt-bridges start loosing their stability in presence of phospholipids. Especially, the tendency of separation of C-terminal domain increases as we spatially move from salt-bridge 1 to 5, highlighting the fact that the C-terminal domain has a higher propensity to loose contact from N-terminus domain at region 5 than at the region 1. Figure S2 establishes this varying tendency of the different salt-bridges to open-up. The Salt-bridge 5 having a peak at larger distance signifies that it has a higher opening tendency and as we move towards salt-bridge 1, this propensity continues to decrease. The role of intrinsically disordered regions (IDR) (residues 1-11 , 181-187, 198-209, 224-235, 264-299) in stabilising the tertiary fold of apoE3 has been previously emphasised by structure-based investigations.[57] Our current simulation trajectories involving lipid particles and apoE3 reveal that, upon assembly of lipids around the protein, these IDRs gradually move away from the N-terminal helix bundles. The intrinsically disordered regions of the protein tend to loose contact with the bundle of 4 helices of the N-terminal domain which is reflected in their collective radius of gyration (figure 4c). The progression of increasing

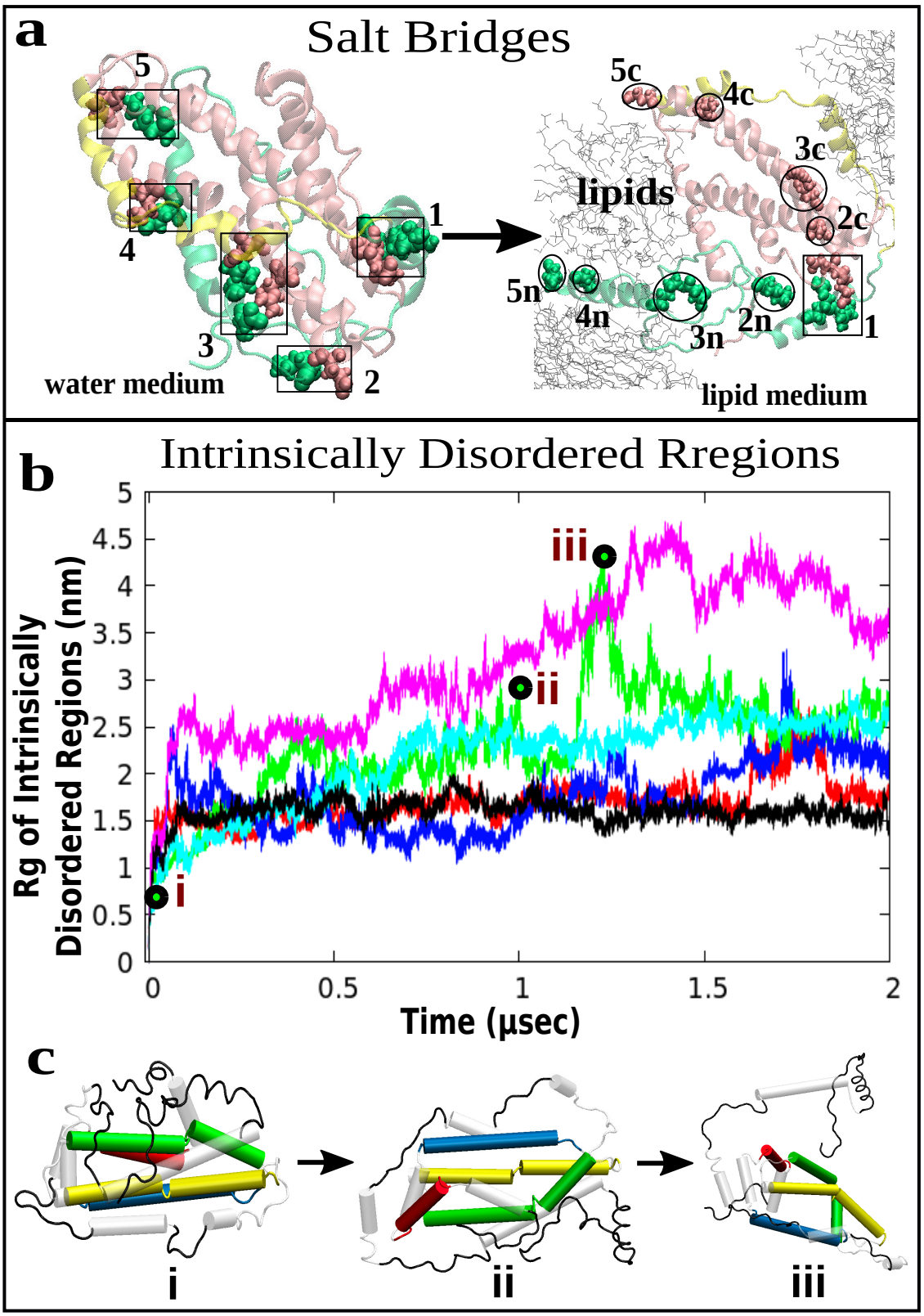

Figure 4: The effect of lipid-assembly on apoe3 structure: **a.** The disruption of salt-bridges 1-5 due to exposure to lipids **b.** Time series of radius of gyration of the intrinsically disordered regions of the protein for different trajectories. **c.** The snapshots at multiple time-points highlighted in the part b of the figure.

radius of gyration of the IDRs (figure 4b) and the accompanying snapshots at different time points (figure 4c) elucidate the overall process of dissociation of IDRs upon the unfolding of C-terminal domain.

2. Slow lipid-induced unfolding of N-terminal domain as the final stage

2A. Coarse-grained simulation captures slow unwinding of N-terminal domain: Results in the previous section showed that our multi-microsecond long atomically detailed simulations were able to capture the lipid-induced reorganisation process of C-terminal domain of apoE. However, N-terminal domain of the proteins remained largely unperturbed by lipids within the micro-second long time scales of the all-atom simulations. Accordingly, we inferred that any further conformational organisation of the apoE might require exploring the conformational phase space for a longer time scale. Modelling with coarse-grained force-fields helps one in reducing the number of degrees of freedom and choosing a larger time-step[58,59] to integrate the equations of motion. This prompted us to adopt a coarse-grained model of the protein-lipid mixtures so as to facilitate the access of relatively longer simulation time scale. Towards this end, the equilibrated configuration as obtained from the all-atom MD simulations, in which C-terminal domain has been completely separated from the N-terminal domain, served as the initial conformation for our coarse-grained simulation. We employed MARTINI force field[60–64] to map the atomistic conformations of apoE3, DPPC lipids and water into their respective coarse-grained representations. Figure 5a represents the initial conformation of protein-lipid complex (with C-terminal domain separated) mapped in coarse-grained representation. Supplemental movie S2 (see link `https://www.dropbox.com/s/3u6kty5rahh4ork/movie_S2.mp4?dl=0`) and movie S3 (see link `https://www.dropbox.com/s/pjjo90g8lfboewe/movie_S3.mp4?dl=0`) depicts the dynamical process of conformational reorganisation, as observed in a pair of 30-microsecond-long independent coarse-grained trajectories. We find that all helices of N-terminal domain

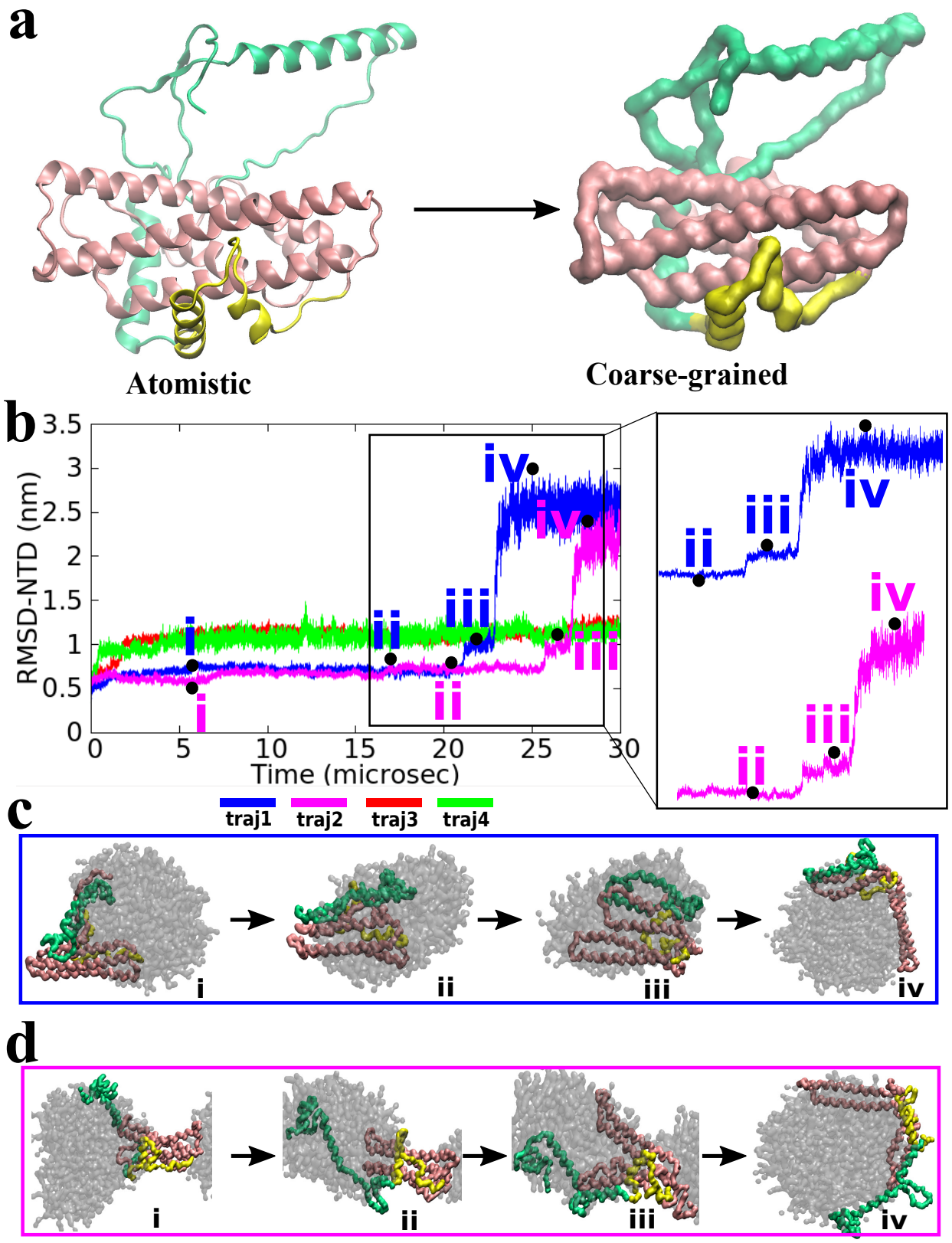

Figure 5: **a.**Coarse-graining of all-atom model of apoe3 (obtained at the end of 2-microsecond long apoe3-lipid all-atom simulation) for exploring long time scale apoE-lipid interaction behaviour. **b.** The time series of RMSD of N-terminal domain (NTD) with respect to the initial conformation of the coarse-grained MD simulation. **c.**Four important snapshots from trajectory-1. **d.** Four important snapshots from trajectory-2. In both these trajectories, the NTD open up with the helices 1-2 separate apart from helices 3-4. (refer to the color code described in the figure 1)

remain fairly closed to each other for a long part of coarse-grained simulation time, while the C-terminal domain remains separated. However, after sampling an ensemble of close-packed N-terminal domain conformation for a long time, helix1/helix2 of N-terminal domain start getting separated from helix3/helix4 and the lipid molecules start invading the resulting intermediate gaps between these two sets of helices of N-terminal domain.

2B. The mechanism triggering the lipid-induced opening of N-terminal domain: To characterise the lipid-induced conformational organisation of the N-terminal domain, we compute the time profile of RMSD of N-terminal domain during the coarse-grained simulations (figure 5). We find that in two out of four trajectories, each spanning 30 microsecond, the RMSD of N-terminal domain remains low (figure 5b) for a large duration of the simulation, until it shows sharp increase at around 20-25 microsecond, thereby suggesting the onset of sudden conformational organisation of N-terminal domain. Parts c and d of figure 5 represent the key conformations from different time point of coarse-grained simulation trajectories: the gradual lipid-induced opening of N-terminal domain is quite evident in the snapshots from these trajectories. The two trajectories capturing the complete opening of the helix1/helix2 and helix3/helix4 are represented by blue and magenta curves in their respective N-terminal domain's RMSD profile. The profile suggests that, starting with conformation similar to snapshot I (see figure 5), the opening of N-terminus domain happens in stage-wise manner. Snapshot II and Snapshot III shown in figure 5 for both trajectories are characterised as the early-stage and late-stage intermediate conformations seeding the opening process in both the trajectories and snapshot IV is the eventual conformation with completely separated N-terminal domain.

In a bid to dissect the key residues mediating the process of unwinding of N-terminal domain, we probe the distance between the centre of mass of residues 45-54 and residues 124-129, with the progression of simulation. These two residue-sets (coloured black in figure 6) act as the linker between N-terminal helices 1/2 and helices 3/4 respectively. As shown in figure 6, the distance between the linkers mostly remain trapped within 1 nm until 20

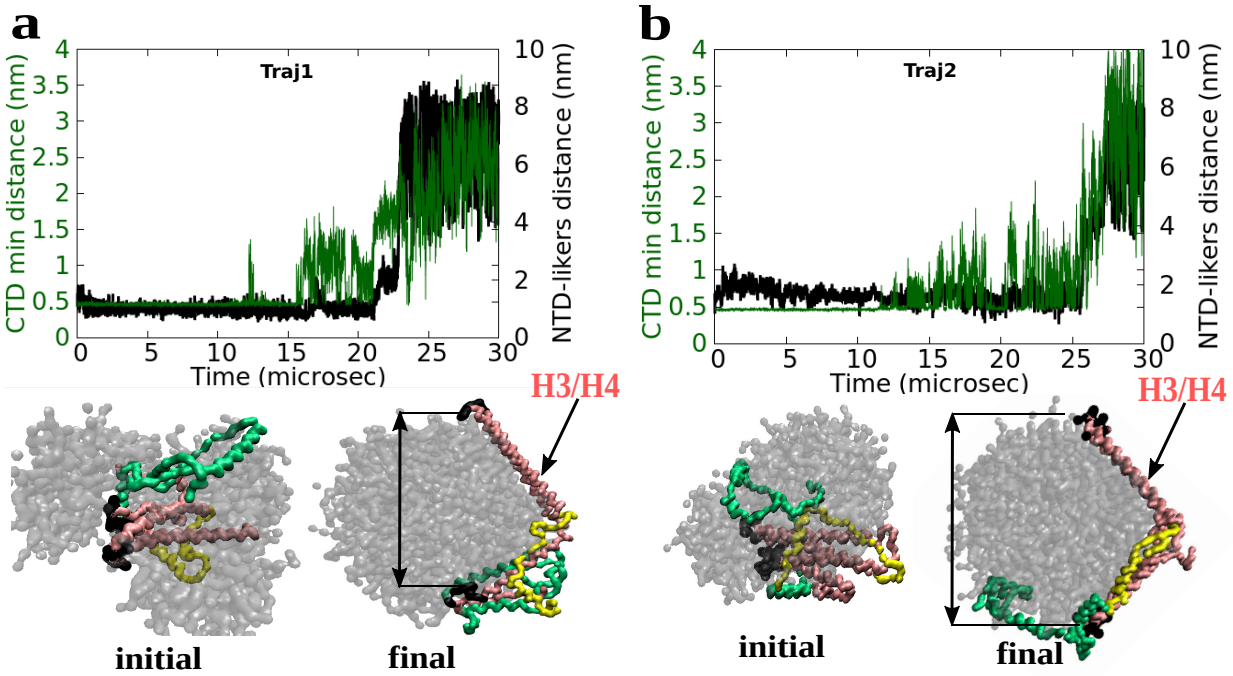

Figure 6: Dissecting the key determinants of lipid-induced unwinding of N-terminal domain in coarse-grained simulation: **a.** For trajectory 1: Right hand axis: The time series of the distance (black curve) between the two linker regions (shown in black in snapshot below) of the N-terminal domain (one between the helices 1/2 and the other between helices 3/4) . Left hand axis: The time series of the minimum distance between the CTD and helices 3/4 shown (green curve). **b.** same as in part a but for trajectory 2. Bottom: Shown in the bottom the initial and final structure in each of the trajectories. The extent of opening up of the N-terminal domain has been pointed out by the double-ended-arrow line in the final snapshot for each of the four trajectories.

microsecond, indicating reversible exploration of closed conformation by the ensemble of apoE-lipid complex. However, in two of the trajectories, (traj1 and traj2) the distance between these two linkers show a large jump to a value of 8.5 nm, signalling the opening of the N-terminal domain. On the same figure, the minimum distance between C-terminal domain and helix 3/helix 4 of N-terminal domain is also plotted. We find that the C-terminal domain (shown in green) initially rests on the helix 3/helix 4 of the N-terminal domain (shown in pink). However, with increased residence of lipid molecules in contact with the helices, the distance between C-terminal domain (especially set of non-polar residues in 227-240 and 280-298) and helices 3/4 starts gradually increasing (figure 6, right axis) in two out of the four trajectories. The overlay between these two distances in figure 6 clearly indicates that the separation process of helices 1/2 from helices 3/4 is strongly correlated with the separation of C terminal domain from helix3/helix 4 of N-terminus domain. The helices 3 and 4 have been marked in each of the four final snapshots. Interestingly, the RMSD profiles of N-terminal domain and distance profiles of the linker regions of other two trajectories (traj3 and traj4) in figure 5 and 6 respectively, also indicate only a partial increase of RMSD or linker separation; suggesting that the N-terminal domain does not completely open up in these trajectories. The final conformation of all four trajectories are shown in figure S3. These ensemble of conformations with partial to complete opening of N-terminal domain emphasize the inherent sluggishness and reversible nature of the separation process of N-terminal domain of apoE3. Finally, Snapshot IV in the bottom panel of the figure 5 represents the final equilibrated conformation of apoE3.lipid complex.

2C. Comparison of simulated hope.lipid complex morphology with experiments: The final open structure, represented in figure 6 is majorly stabilised by the strong hydrophobic association between lipids and reorganised N- and C-terminal domain. The ultimate question is how realistic is the morphology of the apoe3-lipid complex, as obtained from our simulation? There are large volume of precedent experimental investigations based on crystallography and small-angle X-ray scattering techniques which have proposed a di-

verse range of morphologies for apoe3-lipid complex.[4,52,53,65] The morphology of the complex, as obtained from the current work shows very close resemblance with an earlier proposal of a 'open structure',[4] proposed to be obtained via step-wise unfolding of C-terminal and N-terminal domain. Raussens and coworkers[33] had earlier reported a similar open model for apoE3-lipid complex from their experimental investigations, where they had characterised apoE3 N-terminal Domain structure as having the N-terminal helical bundle opened up without any observable helical structure disruption. The final structure attained at the end of current coarse-grained simulations also conform to these earlier proposed models from experiments. In this regard, Weisgraber and co-worker[11] provides a detailed calculation of the surface properties of N-terminal domain where a similar open structure is reached with four-helices bundle in N-terminal domain reorganised as the pink portion in the figure 7c. However, the current work is the first to capture the complete mechanism of the complexation process of full protein in real time.

Conclusion

The full complexation process of apoe3 and phospholipids, as elucidated in current work's unbiased MD simulation efforts is summarised in figure 7. The simulations reported in the current work elucidate, at a molecular level, a multi-stage reorganisation process of apoE3 tertiary fold in presence of lipids : i) a fast lipid-induced opening of C-terminal domain of the apoE3 from the rest of the protein (as observed in our all-atom simulations), followed by ii) a slow lipid-mediated inter-helix separation within N-terminal domain (as observed in our long coarse-grained simulations). The present work's detailed molecular-level illustration of two-stage conformational reorganisation of apoE in presence of phospholipids in real time, provides solid ground to earlier proposals arising from biochemical experiments[43,46,47] and structure-based hypothesis[55,57] that the complete lipid binding process is unlikely to occur in a single stage.

The observation of preferential binding of lipids to the C-terminal domain of apoe3 in the current simulation is consistent with proposed structural basis of lipid binding in apoE3 by Chen et al[55] and kinetic studies by Garai et al.[28,44] In particular, the simulation identifies residues 243-296 as the prominent lipid binding locations in C-terminal domains. Frieden and coworkers have previously hypothesised about the important role that IDRs and salt-bridges potentially play in maintaining the tertiary fold between N-terminal domain and C-terminal domain of apoE3 in water.[57] The current work quantitatively demonstrates that the lipid-induced disruption of several salt-bridges between N- and C-terminal domains and outward movement of IDRs drive the separation of C-terminal domain from the rest of apoe3. The uncoupling process of helices in N-terminal domain, as observed in our coarse-grained simulations, is found to be very sluggish and mainly guided by weakening of interactions between helix 3/helix4 of N-terminal domain and hydrophobic residues of C-terminal domain by the intercepting lipid molecules.

What might be the functional implication of lipid-induced conformational change of apoE3, as derived in the current investigations? Prior hypothesis suggests that only in the maximal lipid-associated state does apoE3 become adept to act as a ligand for LDL receptor[11,38,53,55] and, hence, the lipid-transport metabolic circuit becomes effective. The two-step lipid complexation mechanism of apoe3-fast C-terminal Domain unwinding and slow N-terminal inter-helix separation, as revealed in the current work and earlier proposed by Chen et al,[55] rules out any possibility of partially lipid-bound or lipid-free apoE3 in its native tertiary fold, acting as ligand for LDL receptors. This pre-requisite of optimal lipid-induced conformational reorganization of apoE3 leading to an 'open conformation' for LDL receptor recognition, has also been proposed in prior experimental investigations including FTIR spectroscopic investigations,[33] fluorescence resonance energy transfer-based experiments,[35] tryptophan fluorescence quenching studies by Vasanthy et al[38] and by Karl H. Weisgraber.[11] Overall, The present data obtained from MD simulation support the view that a lipid binding-induced conformational adaptation of apoE, is an essential feature of

apoE function as a ligand for receptor-mediated endocytosis of plasma lipoproteins.

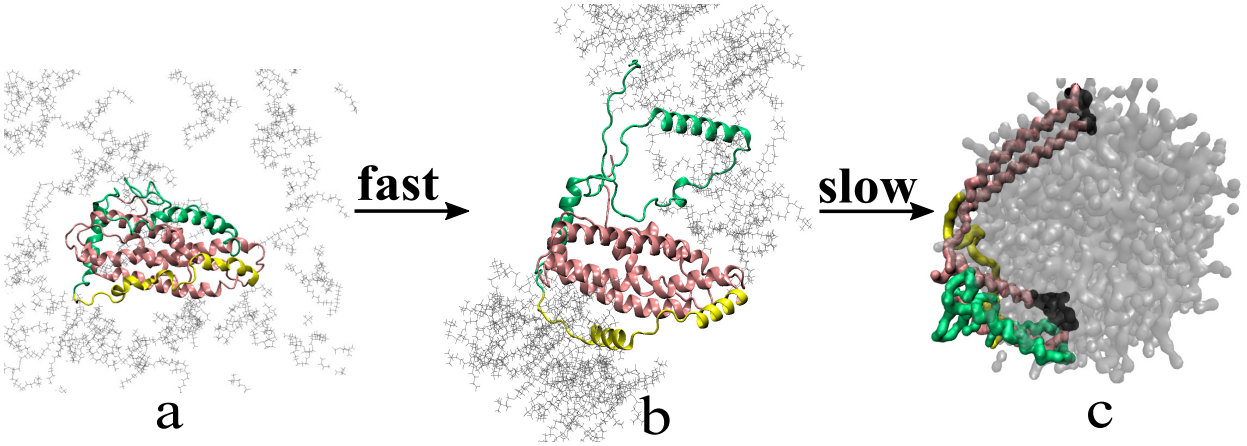

Figure 7: The representative snapshots summarising the overall two-stage opening of apoe3 in presence of phospholipid environment: The atomistic simulations captures the opening up of the green colour C-terminal domain which is a fast process. The slow opening up of the N-terminal domain shown in pink colour is captured in coarse-grained simulation.

The final open structure, represented in figure 6 and figure 8 is majorly stabilised by the strong hydrophobic association between lipids and reorganised N- and C-terminal domain. The ultimate question is how realistic is the morphology of the apoe3.lipid complex ? There are large volume of precedent experimental investigations based on crystallography and small-angle X-ray scattering techniques which have proposed a diverse range of morphologies for apoe3.lipid complex.[4,52,53] However, most of the previous models had been proposed by drawing parallel with the previously proposed model for more popular apoAI-lipid complexes.[43,66] A model of complex involving two biologically active apoE molecules bound to DPPC has also been reported in which each apoE molecule is folded into a helical hairpin.[54] But, many of the models propose dimer of apoe3 to assemble together with lipids. However, more recent conclusion by Garai et al[44] that apoE3 binds to lipid in monomeric form indicates that the any proposal of the apoe3.lipid complex needs to be based on the monomeric apoe3. Towards this end, the current work's report provide a physical ground to the possible morphology of apoE3.lipid complex. The resemblance of morphology of the complex as obtained from the current work provides a solid ground to an earlier proposal of

a 'open conformation'[4] via step-wise unfolding of C-terminal and N-terminal domain.

Methods and Materials:

Atomistic Simulations In our work, all simulation involved single copy of ApoE3 in its monomeric state. The NMR-derived structure of monomeric apoE3 by Chen et al(PDB: 2L7B)[55] formed the basis of all simulation. The protein-only conformation is first energy minimised using steepest descent minimisation scheme. DPPC lipid molecules were randomly distributed around ApoE3. 135 lipid molecules were required to fill the simulation box. 49862 TIP3P[67] water molecules are used to solvate the simulation box and the system was rendered charge-neutral by replacing five water molecules by equal number of potassium ions. A periodic box was implemented with the box dimension of the equilibrated system in each direction equal to 11.92 nm. The entire system was modelled using charmm36[68–71] force-fields. The first step is energy minimization using steepest descent energy minimisation scheme in presence of periodic boundary condition. The energy minimization step is then followed by an equilibration for 100 ps in NVT ensemble at an equilibrium temperature of 320 K using the V-rescale thermostat[72] with time constant 0.1 ps and then equilibrated for 500 ps in NPT ensemble at equilibrium temperature of 320 K using the V-rescale thermostat with a time constant 1 ps and the equilibrium pressure of 1 bar using the Parrinello-Rahman[73] barostat with time constant 0.1 ps using isotropic pressure coupling. All hydrogen bonds were constrained using LINC[74] algorithm and the water molecules were kept rigid using SETTLE algorithm.[75] Six realisations of system , differed by initial velocities, was then propagated for at least 2 μ second using leap-frog algorithm with an integration time step of 2 femtosecond. As a control simulation, a lipid-free simulation of apoE3 in neat water was performed using similar protocol. Towards this end, six trajectories are performed for 2 μ second, with randomised initial velocity, in aqueous medium which contained 31267 water molecules with a box size of 9.867 nm and maintaining a temperature of 320 K.

Coarse-grained Simulations

The protein conformation of all-atom simulated trajectories were clustered (see SI) and the cluster centre showing largest separation of C-terminal domain from N terminal domain apoE3, were chosen for coarse-grained mapping and long time simulations. The coarse-grained protein is lipidated with 135 DPPC lipid molecules. MARTINI coarse-grained model[60–64] was used as the force field of choice. The periodic boundary condition was employed and the empty spaces within the box was solvated by 12204 MARTINI non-polarisable water. The system also required 5 potassium ions to neutralise the simulation box. The system was subjected to energy minimisation and NPT equilibration. The Verlet cut-off scheme used was for equilibration as well as MD run. Finally four copies of 30μsec long MD simulation, with integration time step of 30 fs, were employed to evolve the system maintaining a temperature of 320 K. Thermostat used were velocity-rescale[72] for both equilibration and MD run while the barostat used was berendsen for equilibration while parrinello-rahman[73] for MD run. Multiple realisation of the initial conformation was chosen for this purpose.

Supplemental Information

Supporting information with figures comparing residue-wise helicity of apoE3 in presence and absence of lipid molecules , quantification of lipid-induced salt-bridge opening and description of movies. The folder containing all three movies can be accessed via the link (`https://www.dropbox.com/sh/w1rx535n6fyhfxd/AACkrIsYFuanmja7GQ5JNCPpa?dl=0`)

Acknowledgements

We thank Dr. Kanchan Garai for introducing us to the background of topic of current article. This work was supported by computing resources obtained from shared facility of TIFR Centre for Interdisciplinary Sciences, India. JM would like to acknowledge research intramural research grants obtained from TIFR, DAE, India, Ramanujan Fellowship and

Core Research grants provided by the Department of Science and Technology (DST) of India (CRG/2019/001219).

References

(1) Lee, C.-H.; Olson, P.; Evans, R. M. Minireview: Lipid Metabolism, Metabolic Diseases, and Peroxisome Proliferator-Activated Receptors. *Endocrinology* **2003**, *144*, 2201–2207.

(2) Masoro, E. J. Lipids and Lipid Metabolism. *Annual Review of Physiology* **1977**, *39*, 301–321, PMID: 192136.

(3) Hatters, D. M.; Peters-Libeu, C. A.; Weisgraber, K. H. Apolipoprotein E structure: insights into function. *Trends in Biochemical Sciences* **2006**, *31*, 445–454.

(4) Hauser, P. S.; Narayanaswami, V.; Ryan, R. O. Apolipoprotein E: From lipid transport to neurobiology. *Progress in Lipid Research* **2011**, *50*, 62 – 74.

(5) Fisher, C. A.; Narayanaswami, V.; Ryan, R. O. The Lipid-associated Conformation of the Low Density Lipoprotein Receptor Binding Domain of Human Apolipoprotein E. *Journal of Biological Chemistry* **2000**, *275*, 33601–33606.

(6) Hatters, D. M.; Peters-Libeu, C. A.; Weisgraber, K. H. Apolipoprotein E structure: insights into function. *Trends in Biochemical Sciences* **2006**, *31*, 445–454.

(7) Han, X. The role of apolipoprotein E in lipid metabolism in the central nervous system. *Cellular and Molecular Life Sciences* **2004**, *61*, 1896–1906.

(8) Han, X.; Cheng, H.; Fryer, J. D.; Fagan, A. M.; Holtzman, D. M. Novel Role for Apolipoprotein E in the Central Nervous System. *Journal of Biological Chemistry* **2002**, *278*, 8043–8051.

(9) Fan, J.; Donkin, J.; Wellington, C. Greasing the wheels of Abeta0clearance in Alzheimers Disease: The role of lipids and apolipoprotein E. *BioFactors* **2009**, *35*, 239–248.

(10) Laskowitz, D. T.; Horsburgh, K.; Roses, A. D. Apolipoprotein E and the CNS Response to Injury. *Journal of Cerebral Blood Flow & Metabolism* **1998**, *18*, 465–471.

(11) Weisgraber, K. H. In *Lipoproteins, Apolipoproteins, and Lipases*; Anfinsen, C., Edsall, J. T., Richards, F. M., Eisenberg, D. S., Eds.; Advances in Protein Chemistry; Academic Press, 1994; Vol. 45; pp 249 – 302.

(12) Huang, Y. Mechanisms linking apolipoprotein E isoforms with cardiovascular and neurological diseases. *Current Opinion in Lipidology* **2010**, *21*, 337–345.

(13) Saito, H.; Dhanasekaran, P.; Baldwin, F.; Weisgraber, K. H.; Phillips, M. C.; Lund-Katz, S. Effects of Polymorphism on the Lipid Interaction of Human Apolipoprotein E. *Journal of Biological Chemistry* **2003**, *278*, 40723–40729.

(14) Morrow, J. A.; Segall, M. L.; Lund-Katz, S.; Phillips, M. C.; Knapp, M.; Rupp, B.; Weisgraber, K. H. Differences in Stability among the Human Apolipoprotein E Isoforms Determined by the Amino-Terminal Domain. *Biochemistry* **2000**, *39*, 11657–11666.

(15) Shimano, H.; Yamada, N.; Katsuki, M.; Shimada, M.; Gotoda, T.; Harada, K.; Murase, T.; Fukazawa, C.; Takaku, F.; Yazaki, Y. Overexpression of apolipoprotein E in transgenic mice: marked reduction in plasma lipoproteins except high density lipoprotein and resistance against diet-induced hypercholesterolemia. *Proceedings of the National Academy of Sciences* **1992**, *89*, 1750–1754.

(16) Shimano, H.; Ohsuga, J.; Shimada, M.; Namba, Y.; Gotoda, T.; Harada, K.; Katsuki, M.; Yazaki, Y.; Yamada, N. Inhibition of diet-induced atheroma formation in transgenic mice expressing apolipoprotein E in the arterial wall. *Journal of Clinical Investigation* **1995**, *95*, 469–476.

(17) Zhang, S.; Reddick, R.; Piedrahita, J.; Maeda, N. Spontaneous hypercholesterolemia and arterial lesions in mice lacking apolipoprotein E. *Science* **1992**, *258*, 468–471.

(18) Ghiselli, G.; Schaefer, E.; Gascon, P.; Breser, H. Type III hyperlipoproteinemia associated with apolipoprotein E deficiency. *Science* **1981**, *214*, 1239–1241.

(19) Li, H.; Dhanasekaran, P.; Alexander, E. T.; Rader, D. J.; Phillips, M. C.; Lund-Katz, S. Molecular Mechanisms Responsible for the Differential Effects of ApoE3 and ApoE4 on Plasma Lipoprotein–Cholesterol Levels. *Arteriosclerosis, Thrombosis, and Vascular Biology* **2013**, *33*, 687–693.

(20) Kolovou, G.; Daskalova, D.; Mikhailidis, D. P. Apolipoprotein E Polymorphism and Atherosclerosis. *Angiology* **2003**, *54*, 59–71.

(21) Kyrosto, C. R.; Baras, J. S. Studying The Role of ApoE in Alzheimers' Disease Pathogenesis Using A System Biology Model. *Journal of Bioinformatics and Computational Biology* **2013**, *11*, 1342003, PMID: 24131052.

(22) Corder, E.; Saunders, A.; Strittmatter, W.; Schmechel, D.; Gaskell, P.; Small, G.; Roses, A.; Haines, J.; Pericak-Vance, M. Gene dose of apolipoprotein E type 4 allele and the risk of Alzheimers disease in late onset families. *Science* **1993**, *261*, 921–923.

(23) Weisgraber, K. H.; Mahley, R. W. Human apolipoprotein E: the Alzheimer's disease connection. *The FASEB Journal* **1996**, *10*, 1485–1494.

(24) Hauser, P.; Ryan, R. Impact of Apolipoprotein E on Alzheimer's Disease. *Current Alzheimer Research* **2013**, *10*, 809–817.

(25) Mahley, R. W.; Weisgraber, K. H.; Huang, Y. Apolipoprotein E4: A causative factor and therapeutic target in neuropathology, including Alzheimers disease. *Proceedings of the National Academy of Sciences* **2006**, *103*, 5644–5651.

(26) Zhong, N.; Weisgraber, K. H. Understanding the Association of Apolipoprotein E4 with Alzheimer Disease: Clues from Its Structure. *Journal of Biological Chemistry* **2008**, *284*, 6027–6031.

(27) Laws, S. M.; Hone, E.; Gandy, S.; Martins, R. N. Expanding the association between theAPOEgene and the risk of Alzheimers disease: possible roles forAPOEpromoter polymorphisms and alterations inAPOEtranscription. *Journal of Neurochemistry* **2003**, *84*, 1215–1236.

(28) Frieden, C.; Garai, K. Structural differences between apoE3 and apoE4 may be useful in developing therapeutic agents for Alzheimers disease. *Proceedings of the National Academy of Sciences* **2012**, *109*, 8913–8918.

(29) Acharya, P.; Segall, M. L.; Zaiou, M.; Morrow, J.; Weisgraber, K. H.; Phillips, M. C.; Lund-Katz, S.; Snow, J. Comparison of the stabilities and unfolding pathways of human apolipoprotein E isoforms by differential scanning calorimetry and circular dichroism. *Biochimica et Biophysica Acta (BBA) - Molecular and Cell Biology of Lipids* **2002**, *1584*, 9–19.

(30) Strittmatter, W. J.; Weisgraber, K. H.; Huang, D. Y.; Dong, L. M.; Salvesen, G. S.; Pericak-Vance, M.; Schmechel, D.; Saunders, A. M.; Goldgaber, D.; Roses, A. D. Binding of human apolipoprotein E to synthetic amyloid beta peptide: isoform-specific effects and implications for late-onset Alzheimer disease. *Proceedings of the National Academy of Sciences* **1993**, *90*, 8098–8102.

(31) II, B. W.; Convertino, M.; Das, J.; Dokholyan, N. V. ApoE4-specific Misfolded Intermediate Identified by Molecular Dynamics Simulations. *PLOS Computational Biology* **2015**, *11*, e1004359.

(32) Morrow, J. A.; Hatters, D. M.; Lu, B.; Höchtl, P.; Oberg, K. A.; Rupp, B.; Weis-

graber, K. H. Apolipoprotein E4 Forms a Molten Globule. *Journal of Biological Chemistry* **2002**, *277*, 50380–50385.

(33) Raussens, V.; Fisher, C. A.; Goormaghtigh, E.; Ryan, R. O.; Ruysschaert, J.-M. The Low Density Lipoprotein Receptor Active Conformation of Apolipoprotein E. *Journal of Biological Chemistry* **1998**, *273*, 25825–25830.

(34) Feussner, G.; Albanese, M.; Valencia, A. Three-dimensional structure of the LDL receptor-binding domain of the human apolipoprotein E2 (Arg136 → Cys) variant. *Atherosclerosis* **1996**, *126*, 177–184.

(35) Fisher, C. A.; Ryan, R. O. Lipid binding-induced conformational changes in the N-terminal domain of human apolipoprotein E. *Journal of Lipid Research* **1999**, *40*, 93–99.

(36) Mahley, R. W.; Weisgraber, K. H.; Huang, Y. Apolipoprotein E: structure determines function, from atherosclerosis to Alzheimers disease to AIDS. *Journal of Lipid Research* **2008**, *50*, S183–S188.

(37) Mahley, R. W.; Ji, Z. Remnant lipoprotein metabolism: key pathways involving cell-surface heparan sulfate proteoglycans and apolipoprotein E. *Journal of lipid research* **1999**, *40 1*, 1–16.

(38) Narayanaswami, V.; Maiorano, J. N.; Dhanasekaran, P.; Ryan, R. O.; Phillips, M. C.; Lund-Katz, S.; Davidson, W. S. Helix Orientation of the Functional Domains in Apolipoprotein E in Discoidal High Density Lipoprotein Particles. *Journal of Biological Chemistry* **2004**, *279*, 14273–14279.

(39) Lu, B.; Morrow, J. A.; Weisgraber, K. H. Conformational Reorganization of the Four-helix Bundle of Human Apolipoprotein E in Binding to Phospholipid. *Journal of Biological Chemistry* **2000**, *275*, 20775–20781.

(40) Innerarity, T. L.; Friedlander, B. J.; S. C. Rall, J.; Weisgraber, K. H.; Mahley, R. W. Lipid binding-induced conformational changes in the N-terminal domain of human apolipoprotein E. *Journal of Biological Chemistry* **1983**, *258*, 12341–12347.

(41) Innerarity, T. L.; Pitas, R. E.; Mahley, R. W. Binding of arginine rich (E) apolipoprotein after recombination with phospholipid vesicles to low density lipoprotein receptors of fibroblasts. *Journal of Biological Chemistry* **1979**, *254*, 4186–4190.

(42) Peters-Libeu, C. A.; Newhouse, Y.; Hall, S. C.; Witkowska, H. E.; Weisgraber, K. H. Apolipoprotein E•dipalmitoylphosphatidylcholine particles are ellipsoidal in solution. *Journal of Lipid Research* **2007**, *48*, 1035–1044.

(43) Saito, H.; Dhanasekaran, P.; Nguyen, D.; Holvoet, P.; Lund-Katz, S.; Phillips, M. C. Domain Structure and Lipid Interaction in Human Apolipoproteins A-I and E, a General Model. *Journal of Biological Chemistry* **2003**, *278*, 23227–23232.

(44) Garai, K.; Baban, B.; Frieden, C. Dissociation of Apolipoprotein E Oligomers to Monomer Is Required for High-Affinity Binding to Phospholipid Vesicles. *Biochemistry* **2011**, *50*, 2550–2558.

(45) Perugini, M. A.; Schuck, P.; Howlett, G. J. Self-association of Human Apolipoprotein E3 and E4 in the Presence and Absence of Phospholipid. *Journal of Biological Chemistry* **2000**, *275*, 36758–36765.

(46) Mizuguchi, C.; Hata, M.; Dhanasekaran, P.; Nickel, M.; Phillips, M. C.; Lund-Katz, S.; Saito, H. Fluorescence Analysis of the Lipid Binding-Induced Conformational Change of Apolipoprotein E4. *Biochemistry* **2012**, *51*, 5580–5588.

(47) Nguyen, D.; Dhanasekaran, P.; Phillips, M. C.; Lund-Katz, S. Molecular Mechanism of Apolipoprotein E Binding to Lipoprotein Particles†. *Biochemistry* **2009**, *48*, 3025–3032.

(48) RAUSSENS, V.; DRURY, J.; FORTE, T. M.; CHOY, N.; GOORMAGHTIGH, E.; RUYSSCHAERT, J.-M.; NARAYANASWAMI, V. Orientation and mode of lipid-binding interaction of human apolipoprotein E C-terminal domain. *Biochemical Journal* **2005**, *387*, 747–754.

(49) Hatters, D. M.; Voss, J. C.; Budamagunta, M. S.; Newhouse, Y. N.; Weisgraber, K. H. Insight on the Molecular Envelope of Lipid-Bound Apolipoprotein E from Electron Paramagnetic Resonance Spectroscopy. *Journal of Molecular Biology* **2009**, *386*, 261–271.

(50) Narayanaswami, V.; Ryan, R. O. Molecular basis of exchangeable apolipoprotein function. *Biochimica et Biophysica Acta (BBA) - Molecular and Cell Biology of Lipids* **2000**, *1483*, 15–36.

(51) Peters-Libeu, C. A.; Newhouse, Y.; Hatters, D. M.; Weisgraber, K. H. Model of Biologically Active Apolipoprotein E Bound to Dipalmitoylphosphatidylcholine. *Journal of Biological Chemistry* **2005**, *281*, 1073–1079.

(52) Pauw, M. D.; Vanloo, B.; Weisgraber, K.; Rosseneu, M. Comparison of Lipid-Binding and Lecithin:Cholesterol Acyltransferase Activation of the Amino- and Carboxyl-Terminal Domains of Human Apolipoprotein E3. *Biochemistry* **1995**, *34*, 10953–10960.

(53) Raussens, V.; Fisher, C. A.; Goormaghtigh, E.; Ryan, R. O.; Ruysschaert, J.-M. The Low Density Lipoprotein Receptor Active Conformation of Apolipoprotein E. *Journal of Biological Chemistry* **1998**, *273*, 25825–25830.

(54) Peters-Libeu, C. A.; Newhouse, Y.; Hatters, D. M.; Weisgraber, K. H. Model of Biologically Active Apolipoprotein E Bound to Dipalmitoylphosphatidylcholine. *Journal of Biological Chemistry* **2005**, *281*, 1073–1079.

(55) Chen, J.; Li, Q.; Wang, J. Topology of human apolipoprotein E3 uniquely regulates

its diverse biological functions. *Proceedings of the National Academy of Sciences* **2011**, *108*, 14813–14818.

(56) Zhang, Y.; Vasudevan, S.; Sojitrawala, R.; Zhao, W.; Cui, C.; Xu, C.; Fan, D.; Newhouse, Y.; Balestra, R.; Jerome, W. G.; Weisgraber, K.; Li, Q.; Wang, J. A Monomeric, Biologically Active, Full-Length Human Apolipoprotein E†. *Biochemistry* **2007**, *46*, 10722–10732.

(57) Frieden, C.; Wang, H.; Ho, C. M. W. A mechanism for lipid binding to apoE and the role of intrinsically disordered regions coupled to domain–domain interactions. *Proceedings of the National Academy of Sciences* **2017**, *114*, 6292–6297.

(58) Marrink, S. J.; Periole, X.; Tieleman, D. P.; de Vries, A. H. Comment on "On using a too large integration time step in molecular dynamics simulations of coarse-grained molecular models" by M. Winger, D. Trzesniak, R. Baron and W. F. van Gunsteren, Phys. Chem. Chem. Phys., 2009, 11, 1934. *Physical Chemistry Chemical Physics* **2010**, *12*, 2254.

(59) Baron, R.; de Vries, A. H.; Hünenberger, P. H.; van Gunsteren, W. F. Comparison of Atomic-Level and Coarse-Grained Models for Liquid Hydrocarbons from Molecular Dynamics Configurational Entropy Estimates. *The Journal of Physical Chemistry B* **2006**, *110*, 8464–8473.

(60) Marrink, S. J.; Risselada, H. J.; Yefimov, S.; Tieleman, D. P.; de Vries, A. H. The MARTINI Force Field: a Coarse Grained Model for Biomolecular Simulations. *The Journal of Physical Chemistry B* **2007**, *111*, 7812–7824, PMID: 17569554.

(61) Monticelli, L.; Kandasamy, S. K.; Periole, X.; Larson, R. G.; Tieleman, D. P.; Marrink, S.-J. The MARTINI Coarse-Grained Force Field: Extension to Proteins. *Journal of Chemical Theory and Computation* **2008**, *4*, 819–834, PMID: 26621095.

(62) Ingolfsson, H. I.; Lopez, C. A.; Uusitalo, J. J.; de Jong, D. H.; Gopal, S. M.; Periole, X.; Marrink, S. J. The power of coarse graining in biomolecular simulations. *WIREs Computational Molecular Science* **2014**, *4*, 225–248.

(63) Marrink, S. J.; Tieleman, D. P. Perspective on the Martini model. *Chemical Society Reviews* **2013**, *42*, 6801.

(64) de Jong, D. H.; Singh, G.; Bennett, W. F. D.; Arnarez, C.; Wassenaar, T. A.; Schäfer, L. V.; Periole, X.; Tieleman, D. P.; Marrink, S. J. Improved Parameters for the Martini Coarse-Grained Protein Force Field. *Journal of Chemical Theory and Computation* **2012**, *9*, 687–697.

(65) Sivashanmugam, A.; Wang, J. A Unified Scheme for Initiation and Conformational Adaptation of Human Apolipoprotein E N-terminal Domain upon Lipoprotein Binding and for Receptor Binding Activity. *Journal of Biological Chemistry* **2009**, *284*, 14657–14666.

(66) Schneeweis, L. A.; Koppaka, V.; Lund-Katz, S.; Phillips, M. C.; Axelsen, P. H. Structural Analysis of Lipoprotein E Particles†. *Biochemistry* **2005**, *44*, 12525–12534.

(67) Jorgensen, W. L.; Chandrasekhar, J.; Madura, J. D.; Impey, R. W.; Klein, M. L. Comparison of simple potential functions for simulating liquid water. *The Journal of Chemical Physics* **1983**, *79*, 926–935.

(68) Best, R. B.; Zhu, X.; Shim, J.; Lopes, P. E. M.; Mittal, J.; Feig, M.; MacKerell, A. D. Optimization of the Additive CHARMM All-Atom Protein Force Field Targeting Improved Sampling of the Backbone Phi, Psi and Side-Chain Xi1 and Xi2 Dihedral Angles. *Journal of Chemical Theory and Computation* **2012**, *8*, 3257–3273.

(69) Jo, S.; Kim, T.; Iyer, V. G.; Im, W. CHARMM-GUI: A web-based graphical user interface for CHARMM. *Journal of Computational Chemistry* **2008**, *29*, 1859–1865.

(70) Brooks, B. R. et al. CHARMM: The biomolecular simulation program. *Journal of Computational Chemistry* **2009**, *30*, 1545–1614.

(71) Wu, E. L.; Cheng, X.; Jo, S.; Rui, H.; Song, K. C.; Dávila-Contreras, E. M.; Qi, Y.; Lee, J.; Monje-Galvan, V.; Venable, R. M.; Klauda, J. B.; Im, W. CHARMM-GUIMembrane Buildertoward realistic biological membrane simulations. *Journal of Computational Chemistry* **2014**, *35*, 1997–2004.

(72) Bussi, G.; Donadio, D.; Parrinello, M. Canonical sampling through velocity rescaling. *The Journal of Chemical Physics* **2007**, *126*, 014101.

(73) Parrinello, M.; Rahman, A. Polymorphic transitions in single crystals: A new molecular dynamics method. *Journal of Applied Physics* **1981**, *52*, 7182–7190.

(74) Hess, B.; Bekker, H.; Berendsen, H. J. C.; Fraaije, J. G. E. M. LINCS: A linear constraint solver for molecular simulations. *Journal of Computational Chemistry* **1997**, *18*, 1463–1472.

(75) Miyamoto, S.; Kollman, P. A. Settle: An analytical version of the SHAKE and RATTLE algorithm for rigid water models. *Journal of Computational Chemistry* **1992**, *13*, 952–962.